Numerical investigations on a yarn structure at the microscale towards scale transition

P. del Sorbo, J. Girardot *, F. Dau, I. Iordanoff

Institute of Mechanics and Mechanical Engineering (I2M), Dept. Durability of Materials, Assemblies and Structures, Esplanade des Arts et Metiers, 33400 Talence, France

A B S T R A C T

Since the beginning of the last decade, few examples of multifilament models for dry fabrics have been presented in literature. This work deals with the simulation of a single yarn subjected to transverse impact. Inspired by the models previously developed by other authors, a revisited form of Discrete Element Method has been adopted to perform microscopic analyses in a more efficient computational environment. Transverse impact analysis onto a single KEVLAR KM2 yarn has been performed using this approach. Truss elements have been adopted to discretize yarn filaments instead of heavy computational 3D finite elements. A good agreement with literature results has been achieved with an important reduction of computational resource. In the end, a proposed scale transition is discussed.

Keywords:
Yarn
Transversal impact
Ballistic
Numerical modelling
Discrete Element Method
Microscale

1. Introduction

Dry fabrics comprised of high performance materials as Kevlar, Spectra, Zylon and Twaron have been largely adopted in protection systems due to their high penetration resistance and high strength to weight ratio. Some of applications include protecting clothing and containment systems for jet engines.

The outstanding performances of these materials in impact applications are directly related to a large number of parameters which includes fibres mechanical behaviour, weaving type and fibres reciprocal interaction. The energy absorbed by a fabric during an impact could be attributed to a large number of phenomena as fabric acceleration, fabric deformation, friction dissipation by yarn-to-yarn or fiber-to-fibre interactions. All these aspects cannot be individually evaluated using experimental approaches, which are restricted to the evaluation of macroscopic phenomena as penetration or projectile residual speed.

Since their first applications, numerical simulations turned to be a powerful tool to understand and to evaluate mechanical behaviour of dry fabrics under ballistic impact.

Some models assumed the fabric as an homogeneous medium [1–4] while others were based on a mesoscale representation of the structure [5–10].

In the first case, the computational efficiency is preferred to the model accuracy. The discrete nature of the fabric here is not addressed and capturing phenomena as yarn pull-out, individual yarn breakage or inter-yarn friction dissipation becomes difficult or impossible.

In the second case, fabric architecture is explicitly modelled. Representing the yarn individually, it is possible to have a more realistic description of the failure mechanisms near the impact zone and evaluate the effect of yarns interaction.

More recently fibre-level modelling has been adopted for an entire fabric or a part of it [11–14]. Since their high computational requirement, these last models are only justified when microscopic effects, as fibre–fibre interaction or yarn section rearrangement, would be tracked.

The original approach, denoted Digital Element Method, was developed by Wang et al. to simulate weaving processes [15–17]. This method was successively improved by different authors [18,19] and finally extended to impact applications [11,14]. In this specific approach, yarns are modelled as a group of "Digital Fibres". The term "Digital" refers to the fibres section which is larger than reality.

Each "Digital Fibre" was discretized as a sequence of pin-joined trusses while their transversal behaviour was included in the contact model. Usually, a coarse discretization (few dozen of Digital Fibres) was adopted for each yarn.

This method shows considerable improvements in results and phenomena description compared to the mesoscale models, however it relies on some hypotheses that still have to be verified:

* Corresponding author.
E-mail addresses: pietro.delsorbo@ensam.eu (P. del Sorbo), jeremie.girardot@ensam.eu (J. Girardot), frederic.dau@ensam.eu (F. Dau), ivan.iordanoff@ensam.eu (I. Iordanoff).

http://dx.doi.org/10.1016/j.compstruct.2017.05.018

- an elastic equivalence between Digital Fibres and real fibres was established only in longitudinal direction and no information was provided concerning their transverse mechanical behavior as well as the mechanical contact law among fibres. However, it has been demonstrated that inter-fibres contact plays an important role during an impact [12];
- optimum number of Digital Fibers was obtained by a convergence study on the ballistic performance of the whole fabric. This equivalence could fall if the mechanical response of a single yarn is analysed, as the yarns resultant mechanical behaviour is influenced by their reciprocal interaction within the fabrics.

More recently Nilakantan and Sockalingam [13,20,21] approached the filament-level modelling in a more radical way. In these works, a single yarn submitted to transverse impact is analysed. Each fiber of the yarn was considered and modelled using 3D Finite Elements, in order to describe accurately their transverse behaviour. Contact, friction and material anisotropy were considered too. The role of different parameters as fibres transversal stiffness, shear modulus and friction on yarn ballistic performance was exploited. The high computational time, given by the large number of degrees of freedom involved in the simulation, is one of the major drawback of this method. In this work, the same test performed by Nilakantan is reproduced using a revisited version of the Discrete Element Method (DEM) [22]. As in Digital Element Method, each fibre is discretized as a pin-joined sequence of truss elements. However, three main points differentiate it from the works by Wang:

- contact is evaluated using a particle-based approach;
- the multifilament analysis concerns a single yarn instead of a fabric;
- all the 400 fibres are explicitly modeled.

Results of the simulation are then compared to those presented by Nilakantan [13], in order to validate the proposed approach. In the final part a multiscale approach based on the Digital Element Formulation is presented. A comparison between the proposed real scale model and its equivalent "Digital Fibres" model is finally discussed.

2. Yarn transverse impact test

2.1. Test set up

The model consists in a 25.4 mm length Kevlar KM2 600 single yarn clamped at the extremities (Fig. 1) and impacted transversally in the centre by a cylindrical projectile. As in [13], all the 400 filaments which compose the yarn are modelled. Fibres are assumed to be straight and circular with an constant diameter equal to 12 μm. A cylindrical projectile with a mass M of 9.91 mg is located in the centre of the yarn with contact condition at the initial time. Its specific dimensions are a height h of 2 mm and a diameter ϕ of 2.2 mm. The impact velocity V is set to 120 m s^{-1}. Due to the nature of the problem, symmetry conditions are applied. Just half of the yarn is simulated and the original mass of the projectile is divided by two. Moreover, the displacement along the initial yarn axis is imposed to be zero for the yarn centre and for the projectile.

The current work differs from the referenced initial configuration in two details:

- The initial section is supposed to be circular (Fig. 2) with a yarn packing density lower than the hexagonal configuration adopted by Nilakantan. Final results should not be significantly influenced by this difference since a natural redistribution of the fibres is expected under the impact loading;
- Symmetry conditions are introduced, in order to reduce computational time.

2.2. Material properties

Kevlar KM2 is notoriously a transversal isotropic material [23,24]. Since truss elements are used, only longitudinal stiffness here will be considered. Longitudinal Young Modulus E and density ρ are taken equal to 84.62 GPa and 1.44 g cm^{-3} respectively [13,23].

Maximal stress is assumed as failure criterion, with a stress limit σ^{lim} equal to 3.88 GPa. It is worth to notice that the reference author explicitly assumes that failure is only related to the longitudinal stress, since few experimental information are available for the multiaxial failure of these polymeric fibres.

3. Numerical model

3.1. Discrete Element Approach

It has been demonstrated that fabric ballistic performances are strongly influenced by parameters involved in contact mechanisms [25–27,12], then it should be carefully treated in these numerical models. In order to deal efficiently with contact mechanic, a revisited version of the Discrete Element Method (DEM) inspired by the models developed by Wang [11] hereafter is proposed. Discrete Element Method was firstly developed for simulation of granular media by Cundall [28,29]. This method consists in using physical particles, usually rigid, named Discrete Elements (DEs) to discretize a granular system.

More recently, the efficiency of different DEM contact search algorithms have led to an extension of this numerical method to continuous media. Examples of these applications were presented

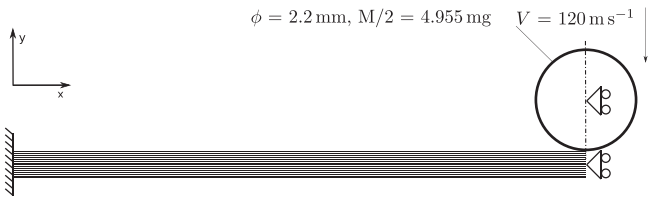

Fig. 1. Transverse impact set up.

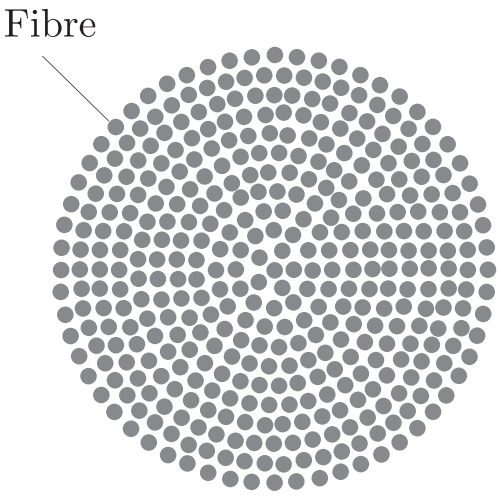

Fig. 2. Initial yarn section layout.

by André et al. [22,30]. In these works the author shows that it is indeed possible to catch a continuous behavior linking the Discrete Elements by mechanical bonds. Thanks to this numerical approach, continuous problems which involve fracture or contact, as composite debonding [31] or concrete failure [32], can be easily adressed without pre-established crack paths.

In the present application a sequence of equally spaced DEs is used to model each fibre of the yarn. These particles carry out the yarn inertial properties and the numerical treatment of contact mechanic, which involves the fibres transversal behaviour. In this first application DEs are considered rigid, therefore a constant displacement field along the fibres thickness will be assumed. In order to represent continuous fibres, deformable trusses have been employed to connect Discrete Elements along the fibres axis. This solution provides a continuum linear displacement field along the fibres longitudinal direction.

According to the model, each Discrete Element can be loaded with two different forces: bond forces and contact forces. Two types of DEs are employed in this simulation. Spherical DEs are used to discretize the fibres while a single cylindrical DE is used to simulate the projectile.

3.2. Filaments discretization

Each fibre is discretized as a sequence of bonded DEs (Fig. 3). Their diameter is assumed to be constant within the model and equal to those of the fibres (12 µm). Bonded DEs are initially equally spaced. Their initial reciprocal distance (the bonds length l_0 in the undeformed configuration) is taken equal to the DEs diameter. Each fibre is discretized by 1059 DEs for a total of 423600 DEs in the entire model. Since the fibres are equally discretized, the global mass of the yarn has been equally distributed within the system. The mass of each DE, denoted m_i, can be evaluated as follow:

$$m_i = \pi \frac{d_{fib}^2}{4} \frac{l}{2} \frac{n_{fib}}{n_{DEs}} \rho, \tag{1}$$

where d_{fib} is the fibre diameter, l is the entire yarn length, n_{fib} is the number of fibres within the yarn and n_{DEs} is the total number of Discrete Elements in the model.

3.3. Bond constitutive behavior

Lets consider a general couple of two Discrete Elements in the framework showed in Fig. 4.

Properties of the first DE will be referred with the index i while properties of the second DE will be referred with the index j. All bonds of the system are modelled as linear trusses. Bond force $\boldsymbol{f}_{ij}^b$ applied by the particle j on the particle i at the time t is computed as follow:

$$\boldsymbol{f}_{ij}^b(t) = k(||\boldsymbol{r}_{ij}(t)|| - l_0)\hat{\boldsymbol{r}}_{ij}(t), \tag{2}$$

$$\text{with } \boldsymbol{r}_{ij}(t) = \boldsymbol{u}_j(t) - \boldsymbol{u}_i(t) \quad k = \frac{EA_0}{l_0}, \tag{3}$$

where $\boldsymbol{u}$ is the position vector of DEs, $\boldsymbol{r}$ is their relative position vector, $\hat{\boldsymbol{r}}$ its unitary vector at time t, E is the Young Modulus of the material in the fibres longitudinal direction, A_0 is the initial area of the fibre section and l_0 is the initial length of the bond.

When a bond reaches the failure stress it is deleted by the simulation:

$$\text{if} \quad \boldsymbol{f}_{ij}^b = -\boldsymbol{f}_{ji}^b \geqslant ||\boldsymbol{f}^{lim}|| = A_0\sigma_{lim} \quad \rightarrow \quad \text{the bond is deleted.} \tag{4}$$

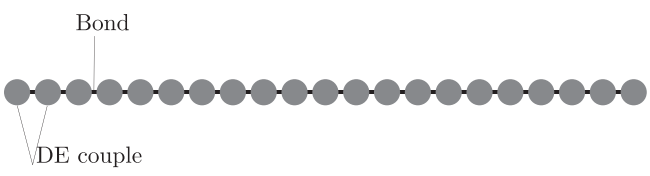

Fig. 3. Fibre Discretization.

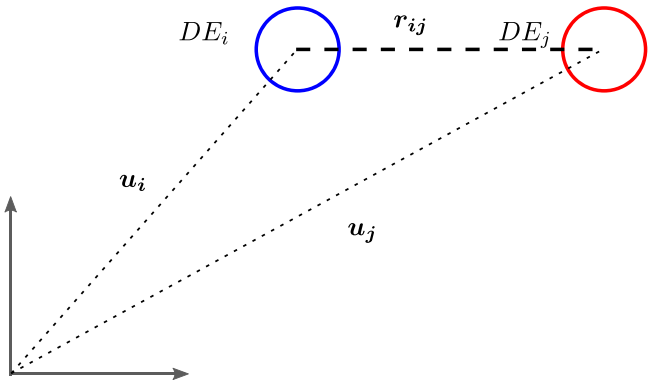

Fig. 4. Framework for the couples of DEs.

3.4. Contact model

3.4.1. Sphere-sphere contact

In this work, a penalty model is used to compute the contact forces among discrete elements. Fibres are assumed to be transversally rigid even if, experimentally, they were found to be elasto-plastic in the transverse direction [23]. When two particles get in contact, a repulsive force $\boldsymbol{f}^c$ proportional to the interpenetration value δ is applied,Fig. 5. The value of the contact force from the particle j on the particle i is:

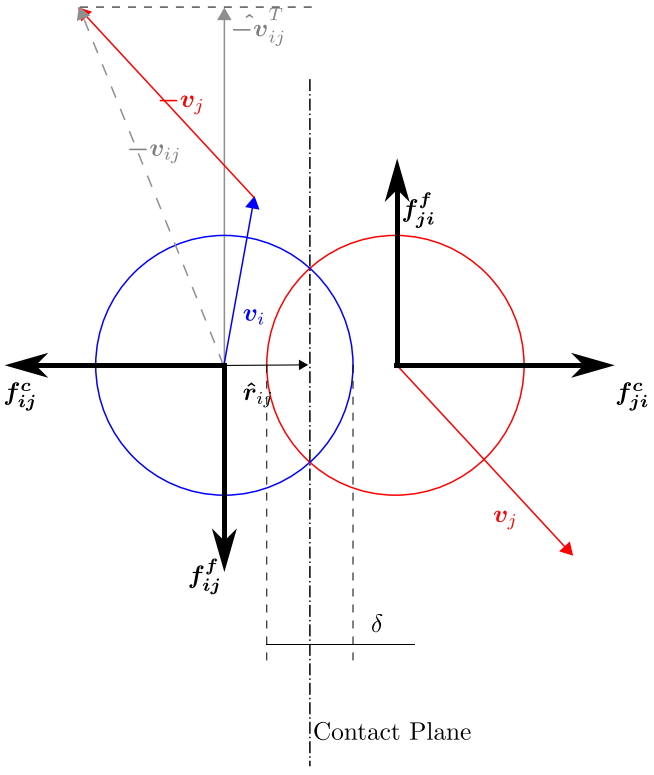

Fig. 5. Framework for the couples of two spherical DEs in contact.

$$\boldsymbol{f}_{ij}^{c}(t) = -k_c \delta \hat{\boldsymbol{r}}_{ij}(t), \tag{5}$$

where k_c is the indentation stiffness which is chosen constant and equal to 500 kN m^{-}. This value is assumed following the parametric analysis in [10] and results to be the best compromise between rigid transversal behaviour and numerical stability of the simulation. It is important to underline that contact has not been activated between bonded elements before bonding failure.

A Coulombian model has been adopted for friction forces $\boldsymbol{f}^{f}$ and gives:

$$\boldsymbol{f}_{ij}^{f}(t) = \mu_f ||\boldsymbol{f}_{ij}^{c}(t)|| \hat{\boldsymbol{v}}_{ij}^{T}(t), \tag{6}$$

where $\hat{\boldsymbol{v}}_{ij}^{T}$ is the unitary vector in the tangential contact plane between DE_i and DE_j (Fig. 5):

$$\hat{\boldsymbol{v}}_{ij}^{T}(t) = \frac{\boldsymbol{v}_{ij}^{T}(t)}{||\boldsymbol{v}_{ij}^{T}(t)||} \qquad \boldsymbol{v}_{ij}^{T}(t) = \boldsymbol{v}_{ij}(t) - [\boldsymbol{v}_{ij}(t) \cdot \hat{\boldsymbol{r}}_{ij}(t)]\hat{\boldsymbol{r}}_{ij}(t) \tag{7}$$

$\boldsymbol{v}_{ij}$ is the relative velocity among the two discrete elements:

$$\boldsymbol{v}_{ij}(t) = \boldsymbol{v}_j(t) - \boldsymbol{v}_i(t) \tag{8}$$

and μ_f, $\boldsymbol{v}_i(t)$,$\boldsymbol{v}_j(t)$ are respectively the kinetic friction coefficient, the velocity of the Discrete Element i and j at the time t. As in the reference test, friction coefficients have been differentiated for fibre–fibre contact and fibre-projectile contact. They have been set respectively to 0.20 and 0.18 [13].

3.4.2. Cylinder-sphere contact

Since a cylindrical projectile has been chosen for the impact simulation, it is necessary to adapt the contact law previously defined to the sphere-cylinder collision, Fig. 6. In this case, the unit vector $\hat{\boldsymbol{r}}_{ij}$ have to be replaced by the unit vector $\hat{\boldsymbol{d}}_{ij}$ directed as the distance between the cylinder axis and the DE_i, using the relation:

$$\boldsymbol{d}_{ij}(t) = \boldsymbol{r}_{ij}(t) - [\boldsymbol{r}_{ij}(t) \cdot \hat{\boldsymbol{e}}(t)]\hat{\boldsymbol{e}}(t), \tag{9}$$

where $\hat{\boldsymbol{e}}$ is the unitary vector parallel to the cylinder axis.

It is worth to underline that contact has been defined just on the cylinder curved face since no contacts are expected on the two ends faces during the simulation.

3.5. Integration scheme

The discrete element model is solved by an explicit integration scheme based on an adapted version of Verlet Velocity algorithm [22]. Total force on a single discrete element $\boldsymbol{f}_i(t)$ is equal to the sum of all the previously mentioned contributions given by its interaction with the entire DEs domain (Eq. (10)):

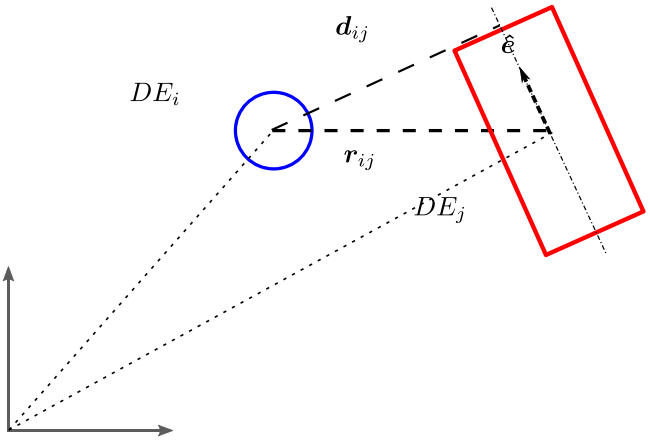

Fig. 6. Framework for the couples of a cylindrical and spherical DEs in contact.

$$\boldsymbol{f}_i(t) = \sum_{j=1, j\neq i}^{n_{DEs}} \boldsymbol{f}_{ij}^{b}(t) + \boldsymbol{f}_{ij}^{c}(t) + \boldsymbol{f}_{ij}^{f}(t). \tag{10}$$

Considering the step time dt, dynamic equilibrium is driven by Eq. (11) and gives the current acceleration $\boldsymbol{a}_i(t)$ as a function of the current total force $\boldsymbol{f}_i(t)$:

$$\boldsymbol{a}_i(t) = \frac{\boldsymbol{f}_i(t)}{m_i} \tag{11}$$

From Verlet Velocity integration scheme, current velocity and position are finally computed using Eqs. (12) and (13):

$$\boldsymbol{v}_i(t) = \boldsymbol{v}_i(t) + \frac{dt}{2}(\boldsymbol{a}_i(t) + \boldsymbol{a}_i(t + dt)), \tag{12}$$

$$\boldsymbol{u}_i(t + dt) = \boldsymbol{u}_i(t) + dt\,\boldsymbol{v}_i(t) + \frac{dt^2}{2}\boldsymbol{a}_i(t). \tag{13}$$

4. Results

4.1. Model validation

Fig. 7 reports the yarn deformed shape at 0 μs(a), 10 μs(b), 25 μs(c) and 40 μs(d).

Classical transverse displacement wave is clearly observed. It begins to propagate when the cylindrical bullet and yarn get into contact and moves leftwards to the clamped edge in the period between 0 μs and 20 μs. When the wave reaches the boundary conditions it is reflected and moves rightwards to the impact point, 20 μs-30 μs. Finally when it reaches the impact point the yarn fails. The so called spreading wave is even observed. This second wave is related to the yarn section rearrangement. When the yarn gets in contact with the projectile, the different fibres spread under the charge and the yarn section changes into a new configuration. This rearrangement of the section travels in the form of a wave in the same direction of the longitudinal wave, Fig. 8.

In order to perform a correct comparison of the results with those of the reference, the first contact among the yarn and the projectile should occur at the same time for both the simulations. The reference author does not report any information about the relative position of the projectile and the yarn in the initial configuration, then a strategy is required to synchronize them. The synchronization has been performed thanks to the internal energy. The instant in which the internal energy starts to grow has been assumed as the initial time for both the simulations. According to this assumption, the reference model has a delay of 2.7 μs on the current one. Fig. 9 reports the history of the projectile velocity compared to the results obtained in [13]. The curves are in very good agreement up to the failure. The relative difference on the residual velocity between the two models is around 6 m s^{-1}, which is closed to 5% compared to the initial speed of 120 m s^{-1}.

A second comparison with the reference model has been performed on the elastic energy Fig. 10. Even in this case, the results of the two models are in good agreement up to the failure initialization. The instant in which the transverse wave is reflected is marked by a dramatic increase of the elastic energy rate. The results are slightly different in the post failure phase. A first difference deals with the shape of elastic energy release. In the current model, it is released more rapidly compared to the 3D FEM. A second difference is in the residual energy. The current model has no residual internal energy after the failure phase while the 3D FEM has a residual one. This could be explained by the lack of bending stiffness of the pin-joined model. After the failure, a large part of internal energy is converted into kinetic one and bending modes become predominant. In this situation, the current model is only able to completely convert the elastic energy in kinetic ones,

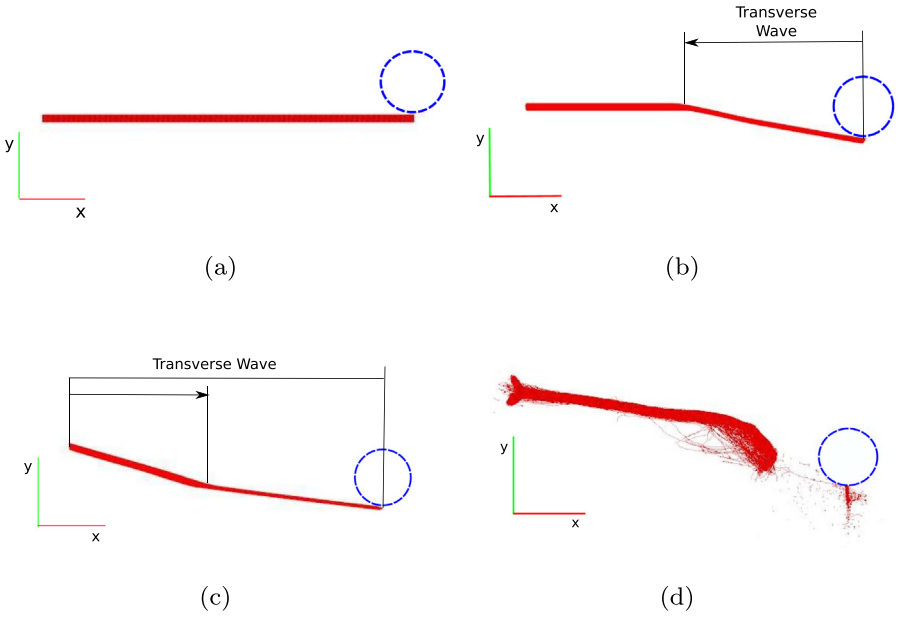

Fig. 7. Impacted Yarn.

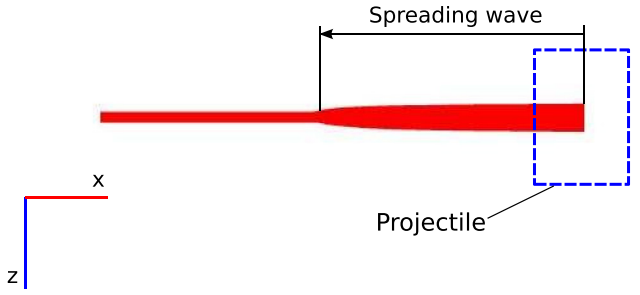

Fig. 8. Spreading wave propagation (10 µs).

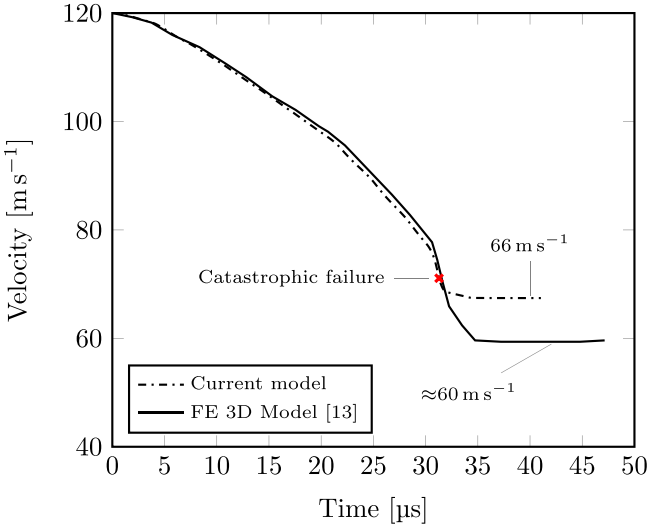

Fig. 9. Projectile velocity comparison for a transverse impact at 120 m s^{-1}.

without restoring it in the bending modes. These differences on the post failure phase could explain the discrepancies in the final speed of the projectile, sign that this phase has an influence on the energy absorption.

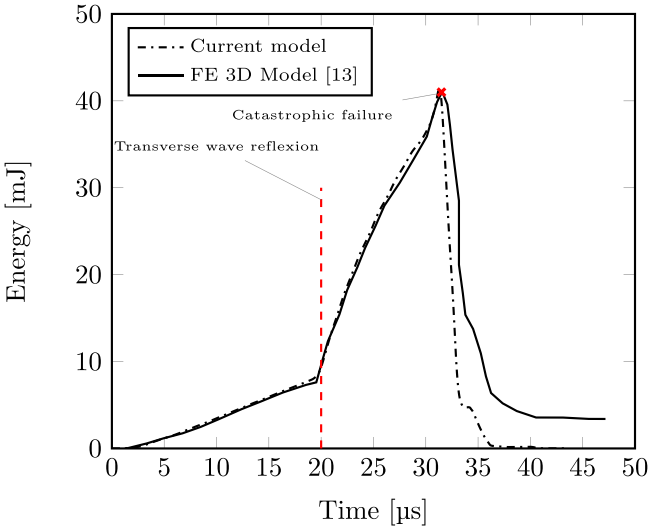

Fig. 10. Elastic energy comparison.

A complete energetic analysis has also been performed. Unfortunately the reference [13] only reports the internal energy for this impact scenario, however a qualitative comparison of the energetic trends could be done with other cases presented in the same work.

Concerning the yarn kinetic energy, it is linearly increasing before the first transverse wave reflection. When transversal wave is reflected, a drastic conversion of kinetic energy into elastic energy is observed. Finally, when catastrophic fail occurs, elastic energy within the yarn is fully converted in yarn kinetic energy.

In the current work, friction dissipation has been divided in two different contributions:

- the first is given by the interaction among the projectile and the fibres and will be denoted as external;
- the second is given by the interaction among the fibres and will be denoted as internal.

As it can be seen on Fig. 11, friction dissipation doesn't play an important role in energy absorption during the impact. It only

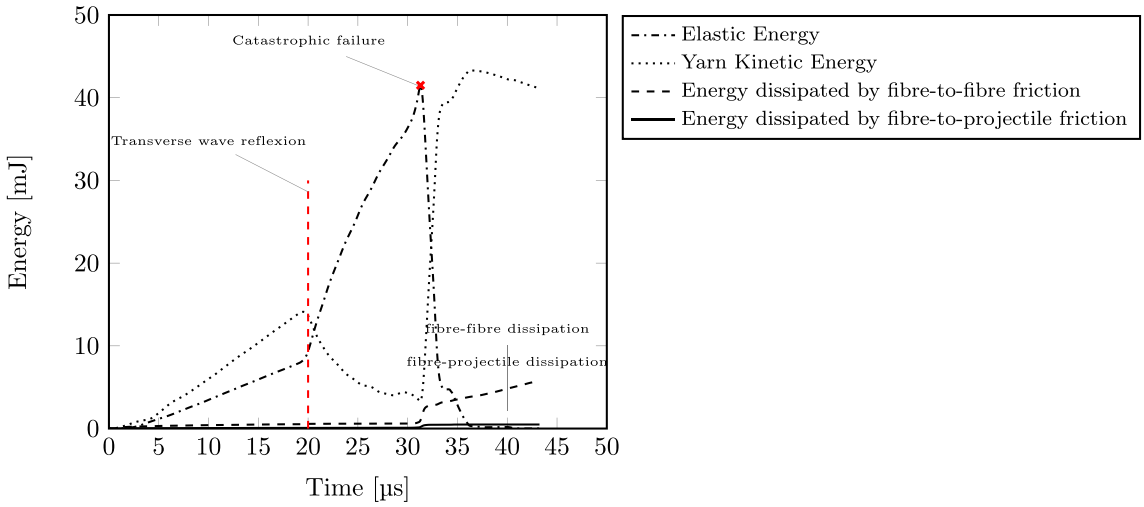

Fig. 11. Energy Balance for a transverse impact at 120 m s^{-1}.

Table 1
Values for the friction coefficients used for the sensitivity analysis.

fiber-projectile friction coeff.	0.0	0.18	0.36
fiber-fiber friction coeff.	0.0	0.2	0.4

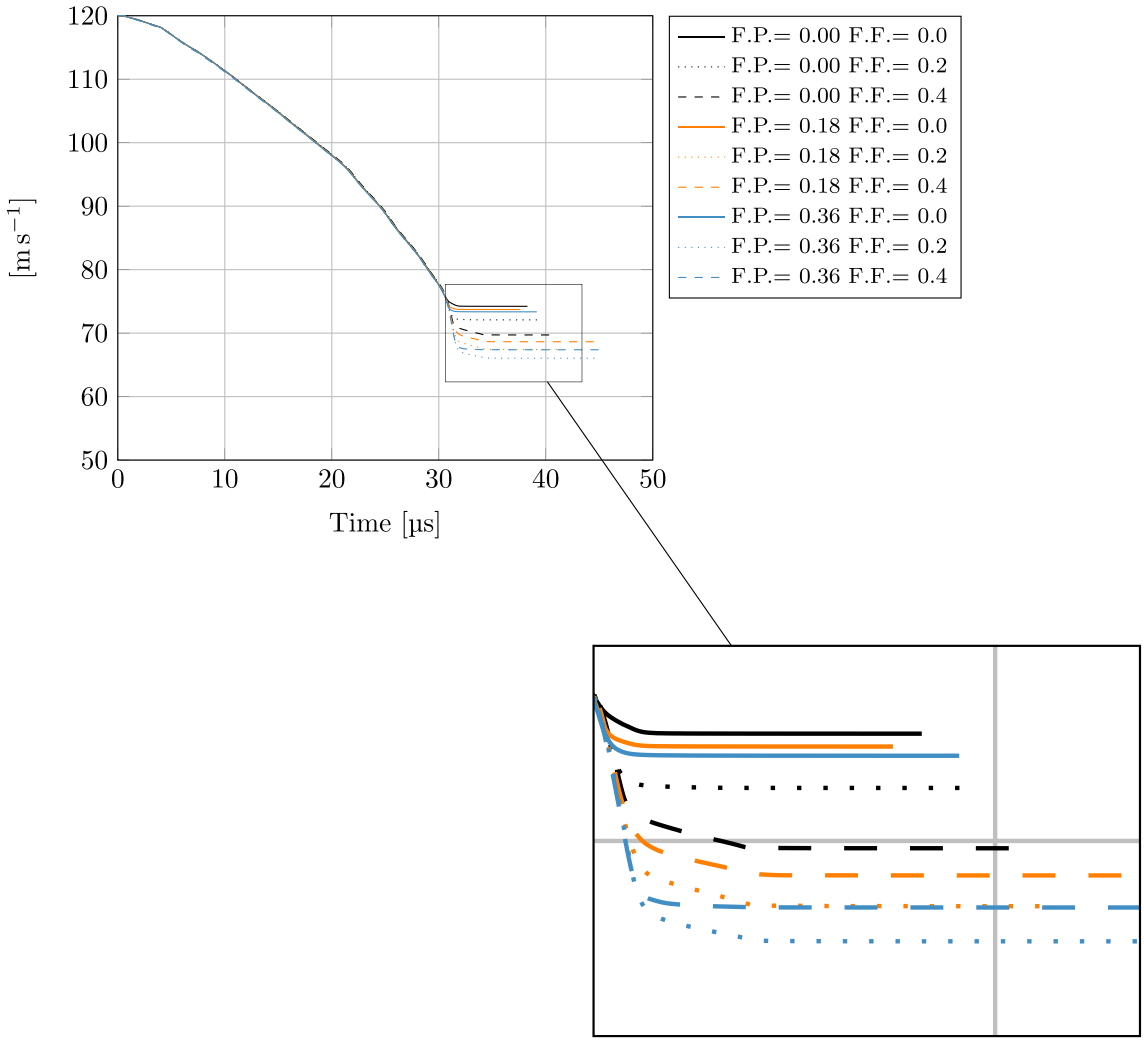

Fig. 12. Effects of friction on projectile velocity (*F.P.* and *F.F.* stand for Fiber-Projectile and Fibre–Fibre friction coefficients).

appears when the system starts to fail. According to the model, internal friction plays a primary role in friction dissipation, however its effects are mostly related to the dissipation of the yarn kinetic energy in the post failure phase.

4.2. Sensitivity analysis on friction coefficients

In order to test the stability of the model and to understand the effect of friction on the transverse impact, a sensitivity analysis on friction coefficient has been performed. Three different values for fiber-to-fiber and fiber-to-projectile friction coefficients have been selected [13] for a total of nine different configurations (Table 1).

The projectile velocity for the nine different cases is reported in Fig. 12. As previously observed by the reference author [13], friction coefficients does not modify the global response of the system but they have a non linear influence on ballistic properties. In particular, fibre-to-projectile friction seems not to have an important effect on the projectile residual speed if no friction among fibres is considered, however a slight increment on fibre-to-fibre friction coefficient leads to some benefits in terms of ballistic performance.

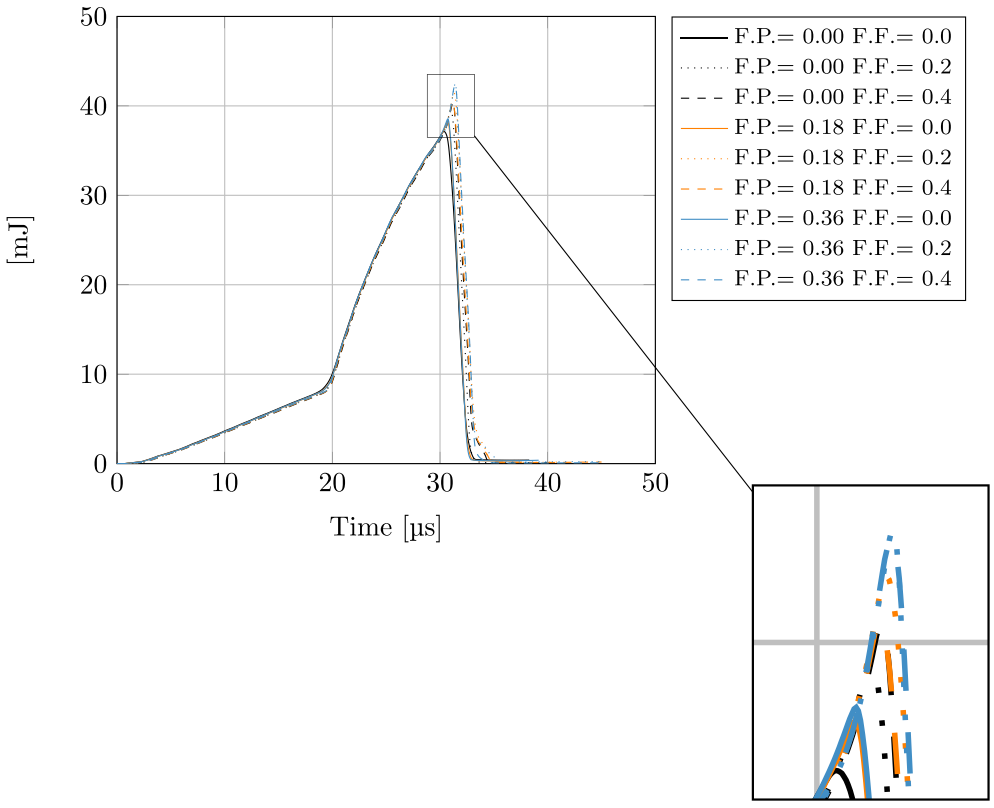

Fig. 13. Effect of friction on the elastic energy.

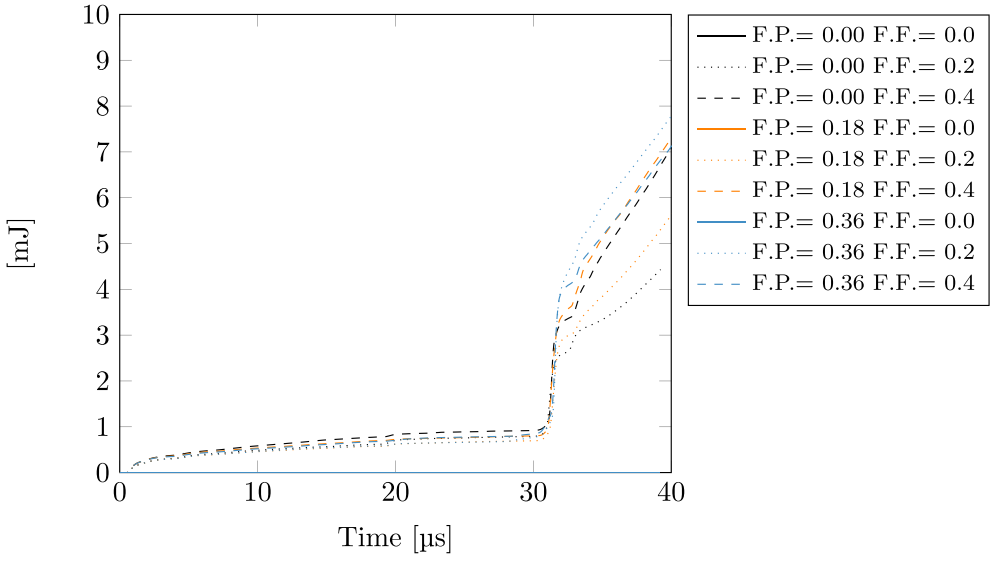

Fig. 14. Energy Dissipated by Fiber-Fiber friction.

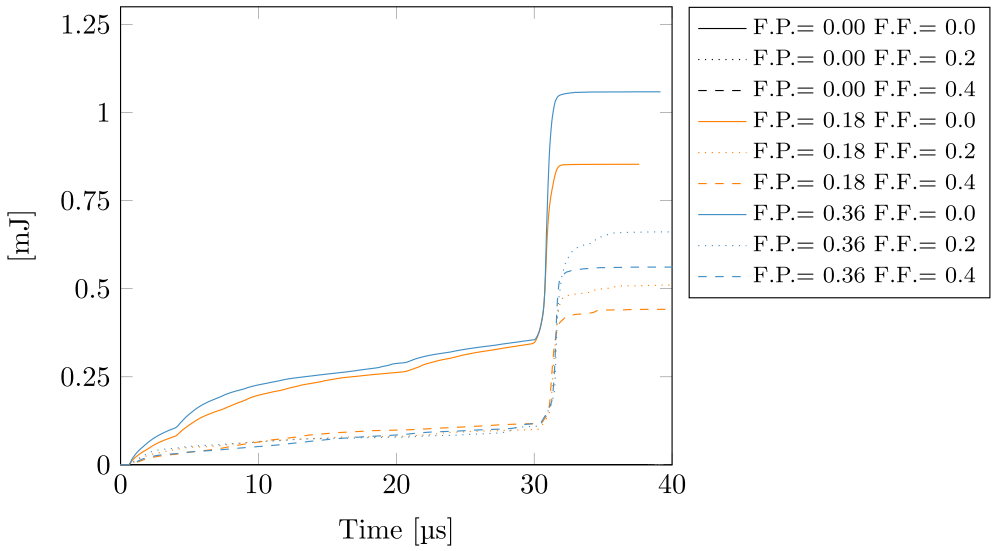

Fig. 15. Energy dissipated by Fibers-Projectile friction.

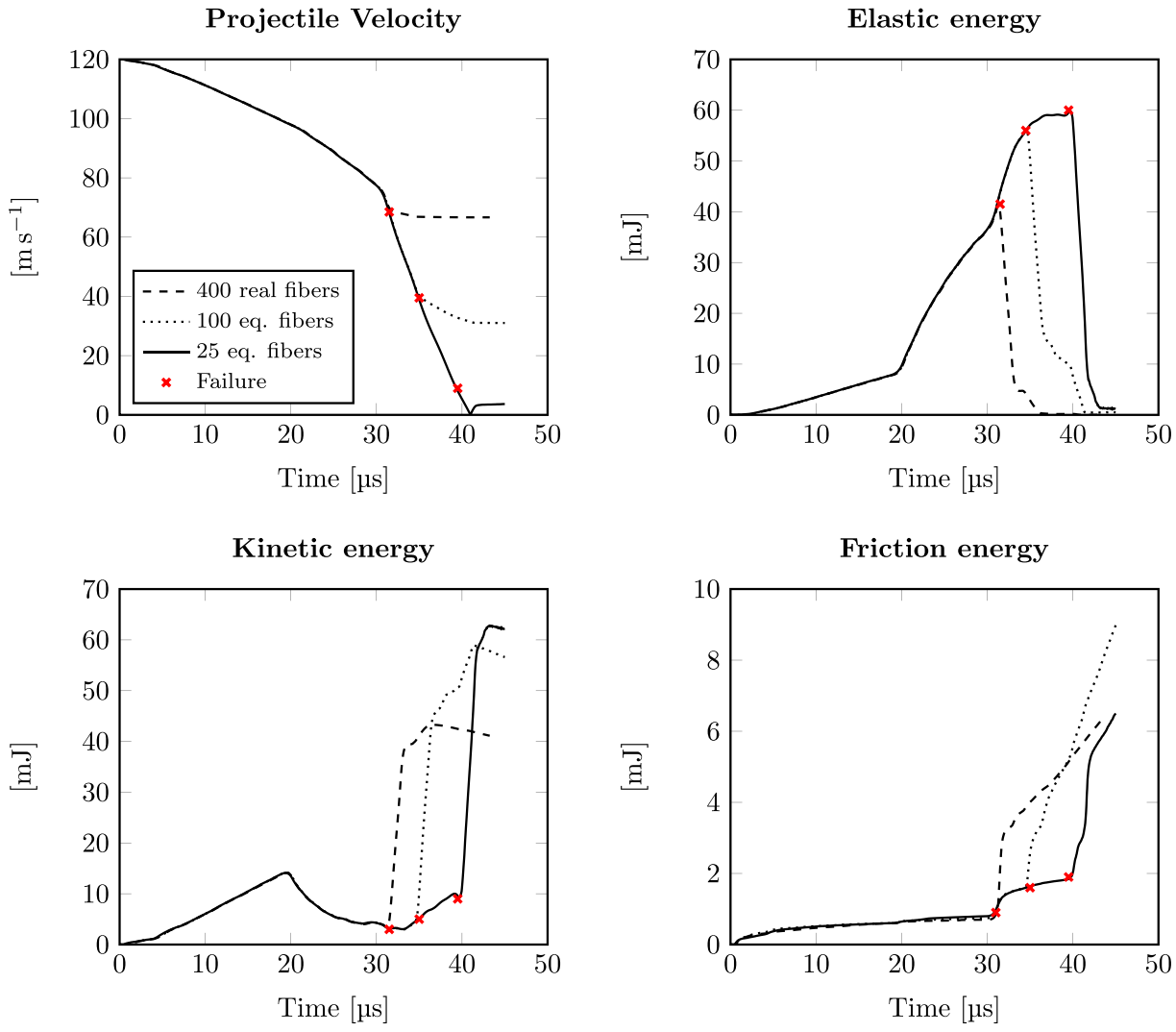

Fig. 16. Energy Balance.

It is worth to notice that the lowest residual speed at 66 m s^{-1} has not been obtained using the highest values of both friction coefficient. This clearly shows a reciprocal interaction among these parameters on the final projectile speed and a reciprocal influence on the failure mechanisms of the structure.

In Figs. 13–15, elastic energy and friction dissipation history are reported for the analysed cases.

A first statement is that friction mostly influence failure initialization. This effect can be observed by the elastic energy trends, Fig. 13, in which failure is delayed for those tests which present an higher value of global dissipation. Global friction dissipation is dominated by the fibre–fibre interactions which are one order higher than the fibre-projectile ones (Figs. 14 and 15). Friction dissipation remains still negligible compared to the other energy forms.A second observation is that friction dissipation is not influenced by friction coefficients before the failure.

4.3. Full to reduced model. A scale transition

In this section, the current model will be compared to the same yarn modelled using an equivalent approach of the Digital Element Method. The full model of 400 fibres is compared with two different models in which yarn is discretized by 100 and 25 longitudinally equivalent "Digital Fibres". Even in this case, fibres are supposed to be straight and circular with a constant diameter. Equivalent radius is determined by the conservation of the yarn volume while the ratio between DEs radius and bond initial length has been kept constant and equal to one. The same contact model and failure criteria adopted for the full model will be used here.

The Fig. 16 compares the results given by these three configurations regarding the projectile velocity and the elastic, kinetic and friction energies. According to these analyses, the global behaviour of the yarn before the failure is well tracked for all the configurations. However, large discrepancies have been found for the failure initialization time. The yarn discretization according to the Digital Element techniques provides a good response of the system even for coarse discretizations (25 Digital Fibres) in terms of macroscopic properties as internal energy, kinetic energy and friction dissipation. However, local effects as failure initialization are closely related to the microscopic nature of the system and to the single fibre properties. These effects drastically influence the ballistic performance of the system, which in some cases has not even been penetrated by the projectile.

5. Conclusion

In this work, the application of a 1D multifilament model to the real scale single yarn modelling has been explored. Kevlar fibres have been modelled by a series of discrete particles relatively connected by truss elements. Those particles are used to deal with the contact according to the Discrete Element Method, while the axial deformation is provided by the bonds between the elements. Results have been compared to those obtained using a multifilament 3D finite elements model and a good agreement with the reference results has been found. The differences between the two models are restricted to the post failure phase when bending modes becomes more relevant. A quantitative analysis of the friction effect on the absorbed energy during the impact has also been performed. As in the results coming from the FEM, friction dissipation appears to be negligible compared to the other energy forms, however it assumes an important role in the failure initialization. The multiscale approach based on the Digital element formulation has been explored at the yarn level. Different questions arise from the equivalence between real scale and equivalent digital fibres. The global response of the systems is well taken into account by both the models, however ballistic performance appears to be dependent on the yarn discretization. Different tests still have to be performed to evaluate the response of these models at the fiber-scale. In further researches, the effect of physical parameters, numerical parameters, impact velocity, projectile shape and element type will be analysed. One important aim of this research path is to take into account the discrete nature of the yarn to the mesoscale. Thanks to this approach it would be possible to clearly capture and understand the failure mechanics of more complex structure as 2D or 3D fabrics.

References

[1] Lim CT, Shim VPW, Ng YH. Finite-element modeling of the ballistic impact of fabric armor. Int J Impact Eng 2003;28:13–31. http://dx.doi.org/10.1016/S0734-743X(02)00031-3.

[2] Ivanov I, Tabiei A. Loosely woven fabric model with viscoelastic crimped fibres for ballistic impact simulations. Int J Numer Meth Eng 2004;61(10):1565–83. http://dx.doi.org/10.1002/nme.1113.

[3] Grujicic M, Bell WC, Arakere G, He T, Xie X, Cheeseman BA. Development of a meso-scale material model for ballistic fabric and its use in flexible-armor protection systems. J Mater Eng Perform 2010;19(1):22–39. http://dx.doi.org/10.1007/s11665-009-9419-5.

[4] Tabiei A, Nilakantan G. Multi-scale ballistic impact simulation of dry woven fabric with elastic crimped fibers. Int J Veh Struct Syst 2011;3(2):74–9. http://dx.doi.org/10.4273/ijvss.3.2.01.

[5] Duan Y, Keefe M, Bogetti TA, Powers B. Finite element modeling of transverse impact on a ballistic fabric. Int J Mech Sci 2006;48(1):33–43. http://dx.doi.org/10.1016/j.ijmecsci.2005.09.007.

[6] Rao MP, Duan Y, Keefe M, Powers BM, Bogetti TA. Modeling the effects of yarn material properties and friction on the ballistic impact of a plain-weave fabric. Compos Struct 2009;89(4):556–66. http://dx.doi.org/10.1016/j.compstruct.2008.11.012. URL http://linkinghub.elsevier.com/retrieve/pii/S1350630711001865.

[7] Ha-Minh C, Boussu F, Kanit T, Crépin D, Imad A. Analysis on failure mechanisms of an interlock woven fabric under ballistic impact. Eng Fail Anal 2011;18(8):2179–87. http://dx.doi.org/10.1016/j.engfailanal.2011.07.011. URL http://linkinghub.elsevier.com/retrieve/pii/S1350630711001865.

[8] Chocron S, Kirchdoerfer T, King N, Freitas CJ. Modeling of fabric impact with high speed imaging and nickel-chromium wires validation. J Appl Mech 2011;78(September 2011):51007. http://dx.doi.org/10.1115/1.4004280.

[9] Nilakantan G, Keefe M, Wetzel ED, Bogetti TA, Gillespie JW. Effect of statistical yarn tensile strength on the probabilistic impact response of woven fabrics. Compos Sci Technol 2012;72(2):320–9. http://dx.doi.org/10.1016/j.compstruct.2011.06.013.

[10] Girardot J, Dau F. A mesoscopic model using the discrete element method for impacts on dry fabrics. Matriaux Techniques 2016;104(4):408. http://dx.doi.org/10.1051/mattech/2016022.

[11] Wang Y, Miao Y, Swenson D, Cheeseman BA, Yen CF, LaMattina B. Digital element approach for simulating impact and penetration of textiles. Int J Impact Eng 2010;37(5):552–60. http://dx.doi.org/10.1016/j.ijimpeng.2009.10.009.

[12] Grujicic M, Hariharan A, Pandurangan B, Yen CF, Cheeseman BA, Wang Y, Miao Y, Zheng JQ. Fiber-level modeling of dynamic strength of kevlar KM2 ballistic fabric. J Mater Eng Perform 2012;21(7):1107–19. http://dx.doi.org/10.1007/s11665-011-0006-1.

[13] Nilakantan G. Filament-level modeling of Kevlar KM2 yarns for ballistic impact studies. Compos Struct 2013;104:1–13. http://dx.doi.org/10.1016/j.compstruct.2013.04.001.

[14] Wang Y, Miao Y, Huang L, Swenson D, Yen C-F, Yu J, Zheng JQ. Effect of the inter-fiber friction on fiber damage propagation and ballistic limit of 2-D woven fabrics under a fully confined boundary condition. Int J Impact Eng 2016;97:66–78. http://dx.doi.org/10.1016/j.ijimpeng.2016.06.007. URL http://linkinghub.elsevier.com/retrieve/pii/S0734743X16303724.

[15] Wang Y, Sun X. Digital-element simulation of textile processes. Compos Sci Technol 2001;61(2):311–9. http://dx.doi.org/10.1016/S0266-3538(00)00223-2.

[16] Zhou G, Sun X, Wang Y. Multi-chain digital element analysis in textile mechanics. Compos Sci Technol 2004;64(2):239–44. http://dx.doi.org/10.1016/S0266-3538(03)00258-6.

[17] Miao Y, Zhou E, Wang Y, Cheeseman BA. Mechanics of textile composites: micro-geometry. Compos Sci Technol 2008;68(7–8):1671–8. http://dx.doi.org/10.1016/j.compscitech.2008.02.018.

[18] Döbrich O, Gereke T, Cherif C. Modelling of textile composite reinforcements on the micro-scale. Autex Res J 2014;14(1):12–7. http://dx.doi.org/10.2478/v10304-012-0047-z. URL http://www.degruyter.com/view/j/aut.2014.14.issue-1/v10304-012-0047-z/v10304-012-0047-z.xml.

[19] Durville D. Simulation of the mechanical behaviour of woven fabrics at the scale of fibers. Int J Mater Form 2010;3(SUPPL. 2):1241–51. http://dx.doi.org/10.1007/s12289-009-0674-7.

[20] Sockalingam S, Gillespie JW, Keefe M. Dynamic modeling of Kevlar KM2 single fiber subjected to transverse impact. Int J Solids Struct 2015;67–68

(May):297–310. http://dx.doi.org/10.1016/j.ijsolstr.2015.04.031. URL http://linkinghub.elsevier.com/retrieve/pii/S0020768315002061.
[21] Sockalingam S, Gillespie JW, Jr, Keefe M, Modeling the fiber length-scale response of Kevlar KM2 yarn during transverse impact doi:http://dx.doi.org/10.1177/0040517516669074.
[22] André D, Iordanoff I, Charles J-L, Néauport J. Discrete element method to simulate continuous material by using the cohesive beam model. Comput Methods Appl Mech Eng 2012;213–216:113–25. http://dx.doi.org/10.1016/j.cma.2011.12.002. URL http://linkinghub.elsevier.com/retrieve/pii/S0045782511003811.
[23] Cheng M, Chen W, Weerasooriya T. Mechanical properties of Kevlar{®} KM2 single fiber. J Eng Mater Technol 2005;127(2):197. http://dx.doi.org/10.1115/1.1857937.
[24] McAllister QP, Gillespie JW, VanLandingham MR. Evaluation of the three-dimensional properties of Kevlar across length scales. J Mater Res 2012;27(14):1824–37. http://dx.doi.org/10.1557/jmr.2012.80.
[25] Duan Y, Keefe M, Bogetti TA, Cheeseman BA, Powers B. A numerical investigation of the influence of friction on energy absorption by a high-strength fabric subjected to ballistic impact. Int J Impact Eng 2006;32(8):1299–312. http://dx.doi.org/10.1016/j.ijimpeng.2004.11.005.
[26] Das S, Jagan S, Shaw A, Pal A. Determination of inter-yarn friction and its effect on ballistic response of para-aramid woven fabric under low velocity impact. Compos Struct 2015;120:129–40. http://dx.doi.org/10.1016/j.compstruct.2014.09.063.
[27] Wang Y, Chen X, Young R, Kinloch I. Finite element analysis of effect of inter-yarn friction on ballistic impact response of woven fabrics. Compos Struct 2016;135:8–16. http://dx.doi.org/10.1016/j.compstruct.2015.08.099. URL http://linkinghub.elsevier.com/retrieve/pii/S0263822315007953.
[28] Cundall P, Strack O. A discrete numerical model for granular assemblies. Géotechnique 1979;29:47–65. http://dx.doi.org/10.1680/geot.1979.29.1.47.
[29] Luding S. Introduction to discrete element methods: basic of contact force models and how to perform the micro-macro transition to continuum theory. 826. Eur J Environ Civ ... (Md) 2008:785. http://dx.doi.org/10.3166/ejece.12.785-826. URL http://www.tandfonline.com/doi/abs/10.1080/19648189.2008.9693050.
[30] André D, Jebahi M, Iordanoff I, Charles J-L, Néauport J. Using the discrete element method to simulate brittle fracture in the indentation of a silica glass with a blunt indenter. Comput Methods Appl Mech Eng 2013;265(8):136–47. http://dx.doi.org/10.1016/j.cma.2013.06.008. URL http://www.sciencedirect.com/science/article/pii/S0045782513001606 http://linkinghub.elsevier.com/retrieve/pii/S0045782513001606.
[31] Yang D, Ye J, Tan Y, Sheng Y. Modeling progressive delamination of laminated composites by discrete element method. Comput Mater Sci 2011;50(3):858–64. http://dx.doi.org/10.1016/j.commatsci.2010.10.022. URL http://linkinghub.elsevier.com/retrieve/pii/S0927025610005811.
[32] Bai Q-S, Tu S-H, Zhang C. DEM investigation of the fracture mechanism of rock disc containing hole(s) and its influence on tensile strength. Theoret Appl Fract Mech 2016;86:197–216. http://dx.doi.org/10.1016/j.tafmec.2016.07.005. URL http://linkinghub.elsevier.com/retrieve/pii/S0167844216300751.